



HAL
open science

Stereoscopic Rendering of Virtual Environments with Wide Field-of-VIEWS up to 360 °

Jérôme Ardouin, Anatole Lécuyer, Maud Marchal, Eric Marchand

► **To cite this version:**

Jérôme Ardouin, Anatole Lécuyer, Maud Marchal, Eric Marchand. Stereoscopic Rendering of Virtual Environments with Wide Field-of-VIEWS up to 360 °. IEEE Virtual Reality, IEEE VR'14, Mar 2014, Minneapolis, Minnesota, United States. hal-00924123v1

HAL Id: hal-00924123

<https://inria.hal.science/hal-00924123v1>

Submitted on 6 Jan 2014 (v1), last revised 8 Jan 2014 (v2)

HAL is a multi-disciplinary open access archive for the deposit and dissemination of scientific research documents, whether they are published or not. The documents may come from teaching and research institutions in France or abroad, or from public or private research centers.

L'archive ouverte pluridisciplinaire **HAL**, est destinée au dépôt et à la diffusion de documents scientifiques de niveau recherche, publiés ou non, émanant des établissements d'enseignement et de recherche français ou étrangers, des laboratoires publics ou privés.

Stereoscopic Rendering of Virtual Environments with Wide Field-of-VIEWS up to 360°

Jérôme Ardouin*
ESIEA - INSA - Inria

Anatole Lécuyer†
Inria - IRISA

Maud Marchal†
INSA - IRISA - Inria

Eric Marchand†
Univ. de Rennes 1 - IRISA

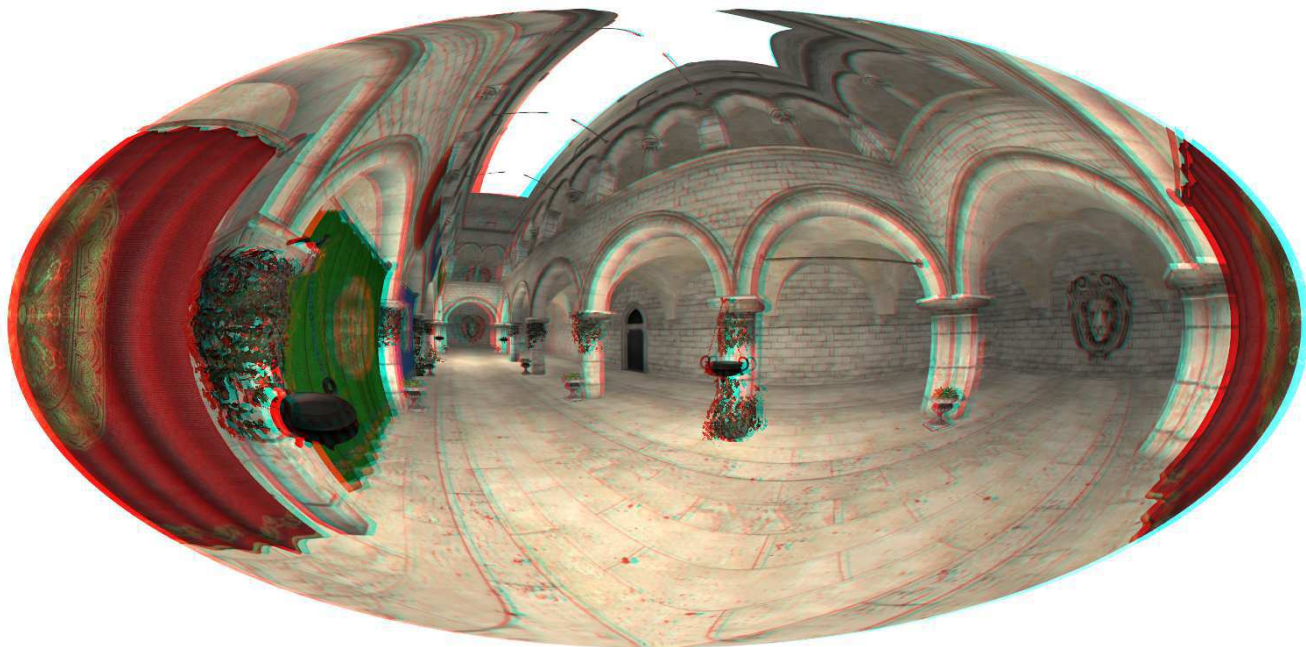


Figure 1: Stereoscopic rendering of a virtual environment covering a 360° horizontal field-of-view. The rendering is based on the Hammer projection which is classically used in cartography. Anaglyph image to be viewed with red/cyan glasses.

ABSTRACT

In this paper we introduce a novel approach for stereoscopic rendering of virtual environments with a wide Field-of-View (FoV) up to 360°. Handling such a wide FoV implies the use of non-planar projections and generates specific problems such as for rasterization and clipping of primitives. We propose a novel pre-clip stage specifically adapted to geometric approaches for which problems occur with polygons spanning across the projection discontinuities. Our approach integrates seamlessly with immersive virtual reality systems as it is compatible with stereoscopy, head-tracking, and multi-surface projections. The benchmarking of our approach with different hardware setups could show that it is well compliant with real-time constraint, and capable of displaying a wide range of FoVs. Thus, our geometric approach could be used in various VR applications in which the user needs to extend the FoV and apprehend more visual information.

Index Terms: H.5.2 [Information Interfaces and Presentation]: User Interfaces—user-centered design; I.3.7 [Computer Graphics]: Three-Dimensional Graphics and Realism—Virtual Reality

*e-mail: jerome.ardouin@esiea-ouest.fr

†e-mail: {alecuyer,mmarchal,marchand}@irisa.fr

1 INTRODUCTION

Many virtual reality (VR) applications require a wide Field-of-View (FoV). A large FoV (i.e. up to 360 degrees) of virtual environments (VE) enables to scan the surroundings and access visual information more rapidly. A panoramic FoV was even found to improve significantly the performance of users during a search and navigate task in desktop VE [2]. However, the rendering of wide FoV VE raises several critical issues [12]. Current approaches are either image-based or geometry-based [17], but often fail at being at the same time: stereo-compatible, GPU-friendly, and able to handle problems related to discontinuities of non-planar projections.

In this paper we propose a novel geometric method for the stereoscopic rendering of VEs with large FoVs, i.e. above 120° and up to 360°, as illustrated in Figure 1. Our method evaluates the non-planar projection equation per vertex, and includes an innovative pre-clip stage in order to solve the problems occurring with polygons spanning across the projection discontinuities.

In the remainder of this paper, we first present related work in real-time rendering using non-planar projections. Then we describe step by step our novel approach to render wide FoV stereoscopic images in real-time. The results and overall performance of our method are reported and discussed in section 5. The paper ends with a general conclusion.

2 PREVIOUS WORK

Several studies concern omnidirectional views of real or virtual environments. As an example, Ardouin et al. designed a device

to augment the human FoV to 360° by processing images from a panoramic sensor [1]. In the VR field, projection-based immersive rooms or Head Mounted Displays (HMD) can immerse the user in a VE with often a large FoV. In almost all cases, visual information of the user’s surroundings is accessed sequentially. To do so, either a head tracker is considered to pan the view within an HMD or several planar screens are used to surround the user (CAVE) [6, 4]. An alternative to planar projection screens is curved surfaces [13] leading to wide screens with cylindrical or dome shape.

If a wide FoV visualization is required on a constrained surface, the rendering method has to rely on non-planar projections, mapping the space directions to the final viewport. The implementation of non-planar projection should use either image-based or geometry-based rendering methods [17].

Image-based approaches render the scene six times with six perspective projections to off-screen textures that are often organized as environment cube map. Then, the final view is rendered by addressing the textures with the desired non planar-projection equations. There are various examples in the literature such as Van Oortmerssen’s FisheyeQuake and PanQuake [18]. Potential drawbacks of such approaches are sampling artifacts or hardware antialiasing/anisotropic filtering incompatibility [9, 12]. Moreover, these methods are not able to generate coherent stereo pairs [15, 16].

Geometry-based approaches can be split into two groups. The first group considers an approximation of non-planar projection with several perspective projections (also known as Perspective Pieces Approximation or PPA). The second group computes the non-planar projection equation per vertex (called Per Vertex Projection Evaluation or PVPE in the remainder of this paper). A classic process to perform PPA rendering is to render the scene geometry n times according to the n perspective projections used to approximate the desired non-planar projection. In [13] this approach is used to adapt single user stereoscopic displays to multi-user scenario. Implementations perform efficiently with a small number of projection pieces [3]. To alleviate saturation of vertex bandwidth when the number of pieces increases, Lorentz et al. proposed a 3-pass rendering method [9]. It replicates the rendered primitive on the GPU and determines which projection pieces the primitive is covering. This approach is characterized by an extensive use of geometry shaders but an alternative implementation using the tessellation unit of modern GPU can also be considered [9]. Stereoscopic rendering can be achieved by rendering the scene two times, translating the projection center for each perspective piece according to the user’s eyes position. However, it still requires a large vertex processing bandwidth which can be a limitation. Alongside the processing pipeline remains difficult to implement on current graphic architectures.

PVPE methods could appear conceptually simpler to design. PVPE is compliant even with early programmable GPUs. Oros proposed a vertex shader implementation that is efficient for FoV inferior to 180° [11]. Alternatively, more complex projections can be used. In [5], a flexible projection can model arbitrary curved viewing volumes. Moreover, the desired non-planar projection can be specifically computed to match spatial arrangement of display surfaces such as in [12]. However, in all cases, two limitations remain. The first is the post-projection error on coarse geometry. The second limitation concern the rendering of primitives crossing a discontinuity of the projection used [12]. These limitations are further discussed in section 3.1.

To the authors’ best knowledge, when considering the different techniques proposed so far in the field of virtual reality it seems that several issues and drawbacks pertain for real-time wide FoV rendering. Thus, in the next section, we propose a technique which remains compliant with projection discontinuity and stereoscopic rendering, scalable, relatively simple to implement (GPU-friendly) and efficient (real-time).

3 A NOVEL APPROACH FOR STEREOSCOPIC RENDERING WITH NON-PLANAR PROJECTION AND WIDE FOV

To solve the technical challenges induced by wide FoV stereoscopic rendering, we propose a novel rendering pipeline that alleviates limitations of PVPE approaches. The successive steps of this pipeline are illustrated in Figure 2.

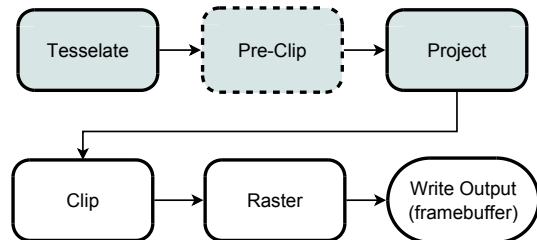


Figure 2: Rendering pipeline proposed for wide FoV real-time rendering. Gray stages are implemented in shaders. The new pre-clip stage (dashed) represents our main contribution.

3.1 Limitations of current PVPE Methods

Per vertex evaluation of non-planar projection seems to be a compelling technique thanks to its compatibility with the standard rasterization pipeline. From a technical point of view, a geometric PVPE approach for wide FoV rendering involves two main steps. First, the geometry is projected into the unit cube. For large FoV, a non-planar projection is mandatory. Second, the transformed primitives are rasterized through scan conversion, i.e. transformation of vectorial data to bitmaps. For performance reasons, the hardware accelerated rasterization pipeline has to be considered, alongside with its restrictions.

Then, the use of non-planar projection induces two major issues. First, the projection does not preserve shapes anymore, leading to important post-projection errors for geometry with low tessellation level. Second, the projection includes discontinuities: if a triangle spans across a discontinuity, it is not properly rasterized. For instance, if we consider a cylindrical equirectangular projection, a triangle spanning across the Oyz half-rear plane, represented by red and blue triangles in Figure 3, is rasterized improperly as shown in Figure 4. The vertices of the polygon are well transformed by the projection equation (their positions after transformation are coherent), but the clipping stage of the standard pipeline is unable to detect and process such kind of polygon. Instead, the primitive is sent as is to the next stage and is rasterized across the viewport. To make up for this issue Petkov et al. [12] propose to simply not render a primitive spanning across a discontinuity of the projection. Alternatively, we propose to include a new clipping stage in the rendering pipeline. This will be presented in section 3.4.

3.2 Building a Projection Suitable for Wide FoV Real-Time Rendering

To be suitable for hardware-accelerated rasterization, a non-planar projection needs to remap the desired view volume to the unit cube. For x and y , the equirectangular projection described in equation (1) is a mapping among others that fits the requirements:

$$\begin{cases} x = \frac{2}{h_{fov}} \lambda \\ y = \frac{2}{v_{fov}} \phi \\ z = -1 + 2 \frac{\rho - near}{far - near} \end{cases} \quad (1)$$

Where $\lambda = \arctan \frac{x}{-z}$, $\phi = \arcsin \frac{y}{\rho}$ and $\rho = \sqrt{X^2 + Y^2 + Z^2}$.

Several other projections can be applied [14]. With Hammer projection (Figure 1), the computation of x and y is more expensive

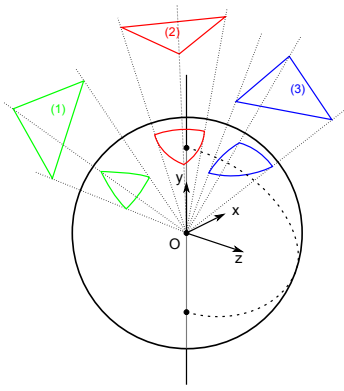


Figure 3: Issues when using an equirectangular projection. The projection discontinuity is represented by the dashed line. Triangle (1) is compatible with standard rasterization. Triangles (2) and (3) generate issues at clipping and rasterization stages.

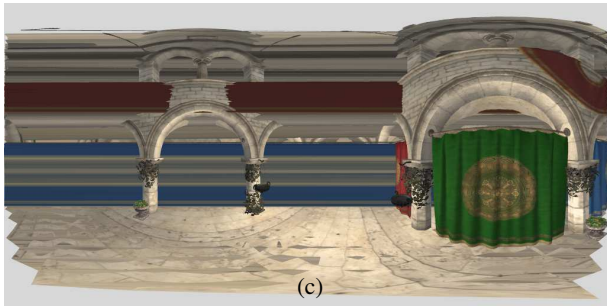
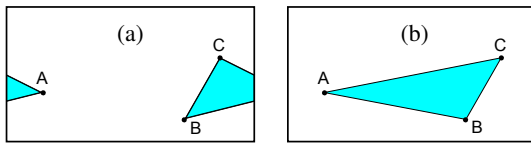


Figure 4: Rasterization issue for triangle projected across the discontinuity of an equirectangular projection. (a): desired rendering in the final viewport. (b): the surface actually generated. (c): the problem on a real scene: here, the triangles composing the red and blue drapes on the very right are rasterized across the whole viewport.

than with the equirectangular projection. When used, it leads to an ellipse shaped view. Note that there are various criteria to prefer or select a specific projection. The shape of the display surface can be considered [12] as well as the properties of the projection used [2]. Conformal projections preserve angles locally. Equidistant and equal-area projections preserve angular distances or surface area. This offers a wide range of possibilities in terms of visual rendering and final perception.

The amount of FoV covered by the final image can be controlled through scalars v_{fov} and h_{fov} . The view volume rendered corresponds to x and y coordinates in $[-1, 1]$. To cover the full FoV, one can choose to use $h_{fov} = 2\pi$ and $v_{fov} = \pi$. Finally, the Z coordinate is generated as the distance from the projected point to the center of projection, also remapped to $[-1, 1]$. To do so, two clip distances are used to define clipping spheres instead of clipping planes used in the perspective case. The whole projection equation is then able to remap the spherical view volume to the unit cube as shown in Figure 5.

3.3 Tessellation of the Virtual Environment Geometry

PVPE approaches require a constraint on the tessellation of the input geometry. An overview of the requirements can be found

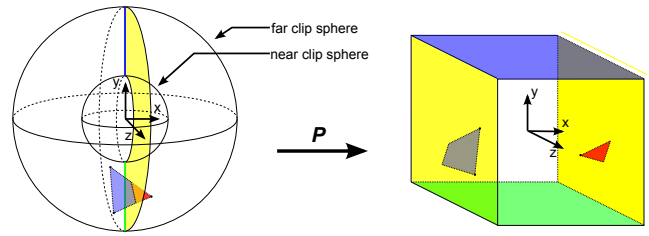


Figure 5: Equirectangular projection used for rasterization. The mapping to the unit cube exhibits discontinuities. Correspondence of surfaces is highlighted with colors (blue, yellow and green). The small triangle (see left image) is cut in two parts. This illustrates the need for a new kind of clipping.

in [12]. Main guidelines are provided hereafter, in order to clarify its inclusion in our rendering pipeline as displayed in Figure 2.

A non-planar projection, such as equirectangular or Hammer projection is built to cover a wide FoV, but introduces distortions in the final view, transforming straight lines into curves, and polygons to curved surfaces. The curvature of the transformed primitive has to be approximated. The granularity of the geometry needs to ensure that the footprint of the primitive after projection is small enough to constrain the projection error. To do so, the geometry can be processed offline before the rendering or online with the tessellation feature available in modern GPU. The both processes can also be applied. Using a tessellation shader in this context offers the possibility, at each rendered frame, to control the way each polygon is subdivided. Primitives suffering from high distortion can be subdivided to a finer level whereas primitive in low distortion area of the projection can remain coarser. Such an approach is described in [12].

3.4 Our Novel "Pre-Clip" Stage

As illustrated in Figures 3, 4 and 5, when using a non-planar projection, problems arise for triangles spanning across a discontinuity of the projection. The standard clipping algorithm is unable to detect and handle these particular cases. To be correctly rasterized, these triangles need to be specifically processed before applying the projection. For FoV smaller than 180 degrees the problem can be avoided by culling polygons behind the center of projection but current implementations targeting FoV above 180 degrees drop the rendering of this kind of triangles [12]. To keep the rendering of these triangles, an alternative solution is to clip them. Considering an equirectangular projection, the additional clipping step has to prevent situations in which a primitive is wrongly rasterized due to a span across the projection discontinuity. Focusing on triangle as input primitive, there are two configurations inducing problems (see Figure 3):

- *Pole triangle*: the triangle spans across the y axis;
- *Rear triangle*: the triangle spans across the rear half part of the Oyz plane.

Our novel approach consists in splitting the primitive in sub-parts that do not span across a discontinuity. The guideline for the algorithm is first to detect if a triangle needs to be clipped. If so, its edges are processed sequentially to detect if one crosses the discontinuity. New vertices are generated on the discontinuity, and their attributes are computed using barycentric interpolation. If needed, the coordinates of the newly generated vertices are slightly corrected to guarantee that the vertex keeps a coherent position after being projected. In the case of equirectangular projection, the x coordinate is forced to keep the same sign as the other vertices composing the generated triangle, as illustrated in Figure 6. The algorithms 2 and 1 describe simplified versions of the algorithms implemented for the rear and pole triangles processing. For readability, it omits barycentric interpolation as well as small correction

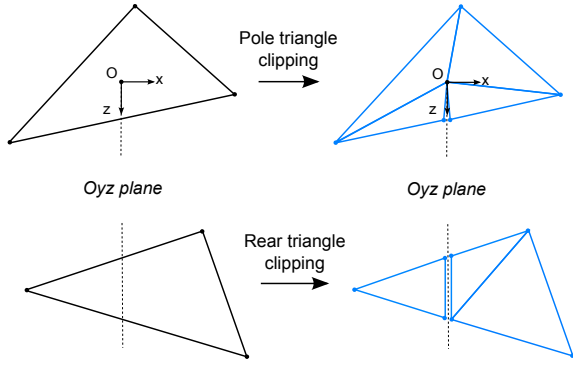


Figure 6: Clipping strategies for pole triangles, projected from top or bottom and spanning across Y axis, and rear triangles, projected from rear half-space and spanning across O_{yz} plane.

Algorithm 1 Pole Triangle Clipping

Input: A triangle T , v_i stands for the i th vertex
Output: A set OT of triangles ready to be projected with an equirectangular projection
if O_y intersects T **then**
 $I \leftarrow \text{computeIntersection}(T, O_y)$
 $id \leftarrow 0$ \triangleright Current ID in vertex list
for $i \leftarrow 0, 2$ **do** \triangleright Check each edge for split
 $VL_{id} \leftarrow v_i$
 $id \leftarrow id + 1$
 $temp \leftarrow \text{OyzIntersect}(v_i, v_{i+1 \bmod 3})$
if $temp$ **then**
 $VL_{id} \leftarrow temp$
 $id \leftarrow id + 1$
end if
end for
for $i \leftarrow 0, 3$ **do** \triangleright Store the 4 triangles
 $OT_i \leftarrow \text{Triangle}(I, VL_{i+1 \bmod id}, VL_{i+2 \bmod id})$
end for
end if

of values introduced to avoid numerical computation errors. Figure 7 illustrates the rendering, after equirectangular projection. The two types of clipping are highlighted: pole triangles are displayed with plain colors and rear triangles with soft gradient colors.

Our approach can comply with any non-planar projection. However the pre-clip stage must be adapted to the discontinuities of the chosen projection. Nevertheless, one strategy for the pre-clip stage can fit for a whole family of projections. For example, the procedure detailed previously fits all cylindrical and pseudo-cylindrical projections [14] such as Hammer projection (Figure 1).

3.5 Computation of a Coherent Stereo Pair and Adaptation to Immersive Displays

To generate coherent images for left and right eyes, the warped volume is considered as a regular object. Therefore, the rendering can rely on classical method used for real-time stereoscopic rendering. Two additional perspective projections are used. First, a zero parallax plane is positioned at the desired distance in the unit cube. It defines the Z where stereoscopic disparity will be null (left and right images are merged). The two centers of projection are positioned according to the desired inter-ocular distance. Near and far clipping planes are also required. They can be chosen to match the unit cube to optimize Z -buffer precision, but this is not mandatory. The final stereoscopic effect can be tuned through three parameters: the inter-ocular distance (iod), the user's distance from the projec-

Algorithm 2 Rear Triangle Clipping

Input: A triangle T , v_i stands for the i th vertex
Output: A set OT of triangles ready to be projected with an equirectangular projection
if O_{yz} intersects T **then**
 $s_0 \leftarrow \text{OyzIntersect}(v_0, v_1)$ \triangleright Compute v_0v_1 edge / O_{yz} plane intersection
 $s_1 \leftarrow \text{OyzIntersect}(v_1, v_2)$
 $s_2 \leftarrow \text{OyzIntersect}(v_2, v_0)$
if s_0 or s_1 or s_2 **then** \triangleright An edge is crossing the O_{yz} plane
 $id \leftarrow 0$ \triangleright Current ID in vertex list
 $ns \leftarrow -1$ \triangleright Handle the non split edge id
for $i \leftarrow 0, 2$ **do** \triangleright Check each edge for split
 $VL_{id} \leftarrow v_i$
 $id \leftarrow id + 1$
if s_i **then**
 $VL_{id} = s_i$
 $id \leftarrow id + 1$
else
 $ns \leftarrow id$
end if
end for
 $OT_0 \leftarrow \text{Triangle}(VL_{(ns+1) \bmod id}, VL_{ns+2 \bmod id}, VL_{ns+3 \bmod id})$
 $OT_1 \leftarrow \text{Triangle}(VL_{ns+3 \bmod id}, VL_{ns+4 \bmod id}, VL_{ns+1 \bmod id})$
 $OT_2 \leftarrow \text{Triangle}(VL_{ns+1 \bmod id}, VL_{ns+0 \bmod id}, VL_{ns+4 \bmod id})$
end if
end if



Figure 7: VE rendered with equirectangular projection. The triangles processed and clipped in the pre-clip stage are highlighted with colors. At the bottom, pole triangles are rendered with solid colors. At the left and right borders, rear triangles that were clipped are rendered with soft colors.

tion plane (d) and the position of the zero-parallax plane in the unit cube ($offset$). After preliminary testings, we could set the values of these parameters to: $iod = 0.5$, $d = 5$ and $offset = -0.8$. Values are given in the normalized device coordinate frame.

There are various display systems that can be used to immerse a user in VEs: HMD, immersive rooms (e.g. CAVE), workbenches, or several other configurations of screens surrounding the user. The method we propose can be adapted to most of these setups. Adapting our method to HMD mainly consists in integrating the data from a three degrees-of-freedom tracker (for head rotations). The data is used to modify the model-view matrix and has no influence on the projection used for the rendering. With immersive displays based on planar projection screens (CAVE, Wall, etc.) the data provided by a tracking system with six degrees-of-freedom needs to be integrated. A straightforward method consists in considering the geometry after the projection as a regular object, fitting the unit cube. This object can then be rendered with classical approach [6], where the tracking data control the center of projection of each perspective

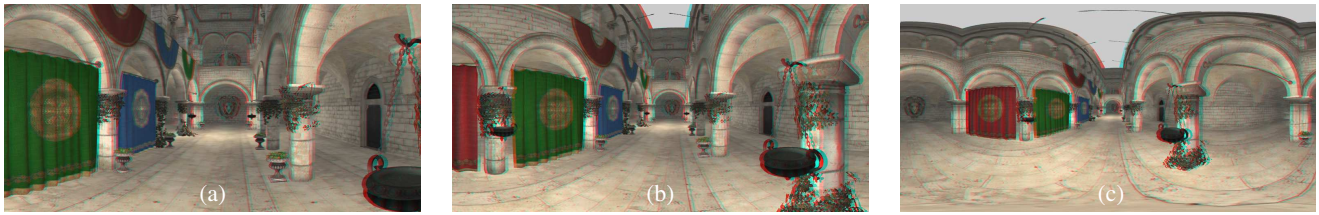


Figure 8: Stereoscopic rendering using equirectangular projection and covering different FoV: (a) 120°, (b) 180°, (c) 360° (Anaglyph images).

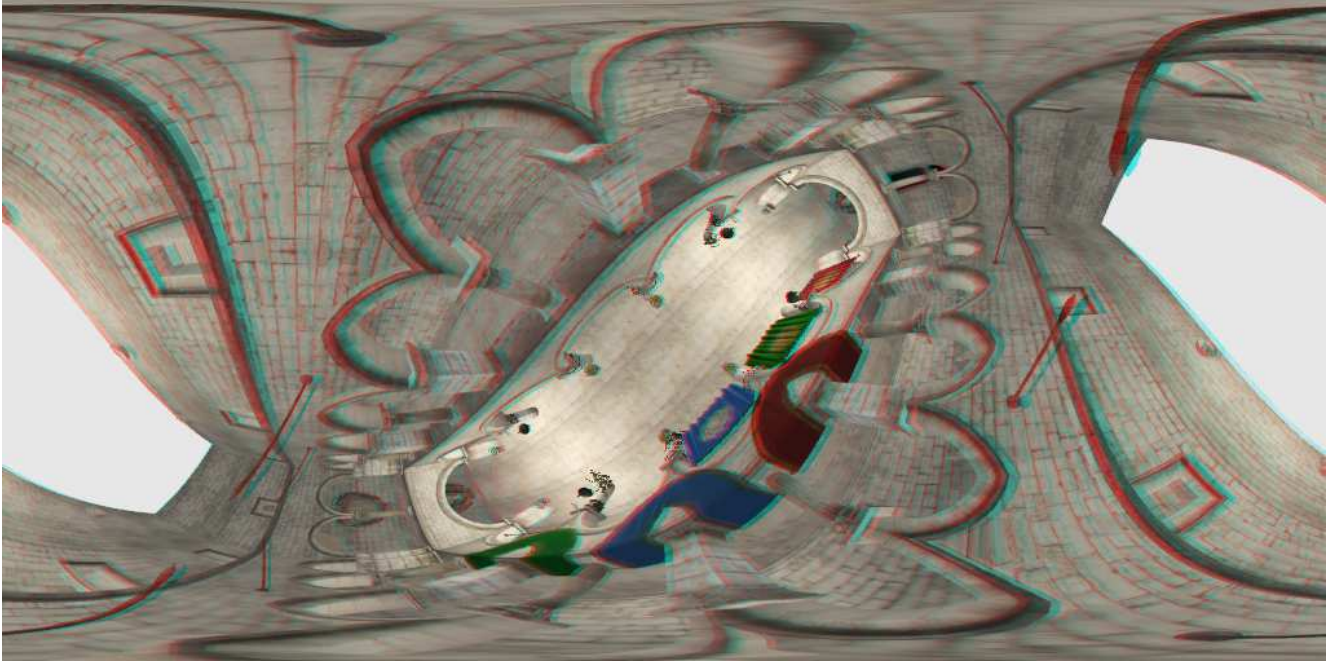


Figure 9: Stereoscopic rendering of the VE viewed from the top and using equirectangular projection (anaglyph image).

projection. Depending on the immersive display targeted, the unit cube may be scaled or translated to match the working area of the display. The method could also be used to target display systems with non-planar screens, such as domes or cylinders [3]. In these cases the non-planar projection should be chosen to match the physical frame of the display. The final image could then be generated in one single pass.

4 IMPLEMENTATION OF THE PROPOSED APPROACH

Our approach was implemented in C++ language using OpenGL 4.2 and the GLSL shading language. The selected VE retained is the Sponza Atrium model [10]. The model was modified offline with a digital content creation tool to subdivide its geometry, offloading the tessellation stage during real-time rendering. All the programmable stages of OpenGL 4.2 pipeline were required to implement the proposed pipeline (Figure 2).

From a sequential point of view, vertices are first transformed in the vertex shader, handling the model-view transformation. Vectorial vertex attributes such as tangents, normals and bi-tangents are transformed with the inverse transpose model-view matrix as in regular rendering. The next step consists in refining the geometry (see details in section 3.3). With the pre-tessellated scene used, a constant level of additional tessellation in the tessellation control shader was found sufficient to limit the projection error. Alternatively, a more optimal algorithm as proposed in [12] could be used. In the next step, the assembled primitives are pre-clipped and projected in the specially designed geometry shader. The pre-clipping algorithm presented in section 3.4 needs to access to the list of the vertices composing the primitive. Therefore, the geometry shader

is the designed place to implement this stage. The primitives are finally transformed with the desired non-planar projection (section 3.2). Concerning the fragment shader implementation, the Phong lightning equation is evaluated in eye space in order to keep the computation independent from the projection. However, deferred shading approach could be used if required [7].

Stereoscopy feature was implemented using two different techniques for image separation: anaglyph (color filter separation, ideal for compatibility and diffusion) and frame sequential (also known as active stereoscopy, for a better viewing experience). The two images were rendered sequentially, in two different drawing passes. Alternatively, layered rendering could be implemented to process the scene only once per frame [17].

5 RESULTS AND DISCUSSION

As a result, our method is able to perform real-time stereoscopic rendering with FoVs up to 360°. Figures 1, 8 and 9 illustrate different examples of stereoscopic images obtained. These images are rendered using anaglyph stereoscopy. Red/cyan glasses are required for viewing. Figure 9 represents a top view of the Sponza Atrium VE. In this particular case, the understanding of the resulting view is not trivial. Distortions in the final rendering and the unusual point of view can mislead the viewer. The addition of stereoscopy seems to ease the perception of the structure and the geometry of the VE. But future work would be necessary to formally assess the potential gain in perception.

The performance of our rendering pipeline was assessed using a standard graphics configuration and a single monitor screen. The test platform runs on Intel i3 2120, running at 3.3GHz, with 4Go

Table 1: Performance of our approach (framerates) as function of FoV, complexity of the VE to render, projection used and usage of anti-aliasing.

| Type of Projection | FoV(°) | Simple VE (fps) | Complex VE (fps) |
|------------------------------|--------|-----------------|------------------|
| Perspective | 120 | 948 | 58 |
| Equirectangular | 120 | 488 | 42 |
| Equirectangular | 180 | 449 | 40 |
| Equirectangular | 270 | 446 | 40 |
| Equirectangular | 360 | 459 | 42 |
| Equirectangular with CSAA32x | 360 | 396 | 36 |
| Hammer | 360 | 476 | 38 |
| Hammer with CSAA32x | 360 | 470 | 39 |

RAM, and an NVidia GeForce 560 GTX graphic board. Vertical synchronization was disabled. Stereoscopic was disabled (multiplying the final performance by nearly two). Rendered viewport sized 1024×512 pixels. Two different projections were tested: equirectangular and Hammer. Two VEs with different complexities were used for the benchmark: the Sponza Atrium [10] as a complex pre-tessellated VE (225839 triangles), and a cornell-box scene as a simple VE (34 triangles). Table 1 displays the resulting framerates, for both VEs, depending on the different FoVs and projections used.

Perspective projection was implemented conserving the pipeline presented in section 3, maintaining all the stages but bypassing the pre-clip stage which is no longer necessary. The results for perspective projection and the equirectangular projection give an estimation of the pre-clip stage impact on framerate. Interestingly enough, several cutting-edge hardware improvements such as antialiasing could be incorporated with small processing-time costs. As an example, hardware antialiasing (CSAA 32x) has been introduced and tested with no visible impact on framerate. Moreover, the FoV extension seems to not influence the rendering performance. In fact, the FoV tuning is available through the mapping to the unit cube (Equation (1)). The main processing duty and the main bottlenecks seem related to the geometry processing steps (clipping and projection) which are implemented in the geometry shader. As our implementation does not feature optimization such as frustum culling, all the geometry is processed whatever the FoV used. So setting a smaller FoV does not imply an augmentation of performances. The fragment processing is here a quite simple standard per-pixel Phong shading that does not seem to impair the final performance.

From the user side, a limitation could be observed concerning the perception of the rendered environments. The human FoV is physiologically limited. Providing more FoV in a view can be viewed as a remapping of a wide FoV to a smaller one, fitting the human natural FoV. This induces a down-scaling of the VE observed. Thus, the perception of scales could become biased, even when using an immersive display. Alongside with the scale perception, perception of depth could be also impaired. However as it can be deduced from section 3.2, the function used to remap the z coordinates can be tuned. This represents a field of investigation to maximize the quality of the final depth and stereoscopic effects. A limitation could be the accuracy of the resulting image in areas of high distortion. Artifacts can be seen in Figure 7 and 8.c: the curvature of the pavement is not regular. Rasterization and interpolation of vertex attributes introduce this bias by using linear interpolation. There are two ways to improve this shortcoming. One way is to augment the tessellation of the VE. In this case, a trade-off between performance and image quality has to be done. Another solution consists in performing rasterization of curved primitives. Such methods exist [8] but are difficult to make efficient (need to enclose the primitive in a bounding shape, discard a lot of fragments...). Future evolution of

hardware could make such approaches more usable by bringing the rasterization stage programmable.

6 CONCLUSION

In this paper, we proposed a novel geometry-based approach for stereoscopic rendering of VEs with a wide field of view. Our approach includes an innovative pre-clip stage to solve problems occurring with polygons spanning across the projection discontinuities. The rendering pipeline complies with current hardware architectures and non-planar projections such as the projections classically used in cartography. Our method has been extended to handle the computation of stereoscopic images and the use of immersive VR systems. The benchmarking of our approach with standard desktop computers and graphics cards could show that it successfully meets real-time performance, and that it is capable of displaying a wide range of FoVs, up to 360° . Therefore, our novel approach could be used in various VR applications in which the user needs to apprehend more visual information, with an extended FoV.

REFERENCES

- [1] J. Ardouin, A. Lécuyer, M. Marchal, C. Riant, and E. Marchand. "Fly-VIZ": A Novel Display Device to Provide Humans with 360° Vision by Coupling Catadioptric Camera with HMD. In *Proc. of VRST*, pages 41–44, 2012.
- [2] J. Ardouin, A. Lécuyer, M. Marchal, and E. Marchand. Navigating in Virtual Environments with 360° Omnidirectional Rendering. In *Proc. of IEEE 3DUI*, pages 95–98, 2013.
- [3] P. Bourke. Synthetic stereoscopic panoramic images. In *Interactive Technologies and Sociotechnical Systems*, Lecture Notes in Computer Science. Springer, 2006.
- [4] D. A. Bowman, E. Kruijff, J. J. LaViola, and I. Poupyrev. *3D User Interfaces: Theory and Practice*. Addison Wesley Longman Publishing Co., Inc., 2004.
- [5] J. Brosz, F. F. Samavati, M. S. T. Carpendale, and M. C. Sousa. Single camera flexible projection. In *Proc. of NPAR*, pages 33–42, 2007.
- [6] C. Cruz-Neira, D. J. Sandin, and T. A. DeFanti. Surround-screen projection-based virtual reality: the design and implementation of the cave. In *Proc. of SIGGRAPH*, pages 135–142, 1993.
- [7] M. Deering, S. Winner, B. Schemdiwy, C. Duffy, and N. Hunt. The triangle processor and normal vector shader: a vlsi system for high performance graphics. In *Proc. of SIGGRAPH*, pages 21–30, 1988.
- [8] J.-D. Gascuel, N. Holzschuch, G. Fournier, and B. Péroche. Fast non-linear projections using graphics hardware. In *Proc. of I3D*, pages 107–114, 2008.
- [9] H. Lorenz and J. Döllner. Real-time piecewise perspective projections. In *Proc. of GRAPP*, pages 147–155, 2009.
- [10] F. Meinl. Sponza model. <http://www.crytek.com>.
- [11] D. Oros. A conceptual and practical look into spherical curvilinear projection. www.frost-art.com.
- [12] K. Petkov, C. Papadopoulos, M. Zhang, A. E. Kaufman, and X. Gu. Interactive visibility retargeting in vr using conformal visualization. *IEEE TVCG*, 18(7):1027–1040, 2012.
- [13] A. Simon, R. Smith, and R. Pawlicki. Omnistereor for panoramic virtual environment display systems. In *Proc. of IEEE VR*, 2004.
- [14] J. Snyder. *Flattening the Earth: Two Thousand Years of Map Projections*. University of Chicago Press, 1997.
- [15] M. Trapp and J. Döllner. Generalization of single-center projections using projection tile screens. In *Computer Vision and Computer Graphics. Theory and Applications*, volume 24 of *Communications in Computer and Information Science*. Springer, 2009.
- [16] M. Trapp and J. Döllner. A generalization approach for 3d viewing deformations of single-center projections. In *Proc. of GRAPP*, pages 162–170, 2008.
- [17] M. Trapp, H. Lorenz, and J. Döllner. Interactive stereo rendering for non-planar projections of 3d virtual environments. In *Proc. of GRAPP*, pages 199–204, 2009.
- [18] W. van Oortmerssen. Fisheyequake. <http://strlen.com/gfxengine/fisheyequake/>.